ISSN 1063-7737, Astronomy Letters, 2014, Vol. 40, No. 10, pp. 606–614. © Pleiades Publishing, Inc., 2014.
Original Russian Text © D.I. Solovyov, O.V. Verkhodanov, 2014, published in Pis'ma v Astronomicheskiĭ Zhurnal, 2014, Vol. 40, No. 10, pp. 671–680.

Radio Galaxies with Signatures of Merging from the List of Giant Radio Galaxy Candidates Based on NVSS Data

D. I. Solovyov[1] and O. V. Verkhodanov[2*]

[1]*Special Astrophysical Observatory, St. Petersburg Branch, Russian Academy of Sciences, Pulkovo, St. Petersburg, 196140 Russia*

[2]*Special Astrophysical Observatory, Russian Academy of Sciences, Nizhnii Arkhyz, Karachai-Cherkessian Republic, 369167 Russia*

Received April 7, 2014

Abstract—Eight radio sources with signatures of interacting galaxies have been detected within the framework of the project aimed at expanding the list of giant radio galaxies based on NVSS data. The objects have a nontrivial structure in the radio band: four sources exhibit an S-shape, three sources exhibit an X-shape typical of sources at the final stage of radio galaxy merging, and one radio galaxy has a double nucleus. Using the CATS, NED, and SkyView databases, we have made the optical and radio identifications of these objects and constructed their continuum radio spectra.

DOI: 10.1134/S1063773714090023

Keywords: *radio galaxies: observations, radio continuum, morphology.*

1. INTRODUCTION

All-sky surveys and open access to archival data allow one to increase the sample and to study the objects of rare morphological types. Several comparatively rarely encountered classes of objects, whose samples should be increased to investigate the population properties, can be identified among the radio galaxies. These include giant radio galaxies, S- and X-shape radio sources, radio galaxies with a submillimeter excess, gravitational lenses, and other objects. The presence of an intense radio emission in radio galaxies is a signature of galaxy merging, which triggered the quasar activity inside the stellar system. The morphology of radio galaxies allows the various activity stages of objects caused by the merging of galaxies and their nuclei to be investigated. One of the observed consequences of the merging process is the precession of the spin axis of the supermassive black hole and the associated jet. This is reflected in the morphological properties of the radio source and manifests itself, for example, as the so-called S-shape of the jet (Wirth et al. 1982; Hunstead et al. 1984; Cotanyi 1990; Sparke and Gallagher 2000; Young et al. 2005). Therefore, expanding the sample of radio objects with S-morphology is extremely important for analyzing the various stages of active nucleus merging.

The X-shape radio galaxies, whose radio brightness distribution in the extended components is not aligned along a single axis but represents the pairs of jets arranged at a comparatively large angle to each other, have a special status among the active objects in the merging process. The number of known objects of this morphological type is ∼150 (Leahy and Williams 1984; Leahy and Parma 1992; Pringle 1996; Murgia 2001; Merritt and Ekers 2002; Wang et al. 2003; Liu 2004). Despite the complexity of their shape, such radio galaxies are mostly classified as FR II radio sources (Fanaroff and Riley 1974) and are identified with giant elliptical galaxies. As a rule, the X-shape radio galaxies have two pairs of widely separated extended components. The active components with a high surface brightness and the so-called "wings" with a lower surface brightness produced by emission from the plasma ejected along the axis of the other jet that does not coincide with the main one are identified in these pairs. According to observational data, the wings often have a larger spectral index and a high degree of polarization (Wang et al. 2003). Leahy and Parma (1992) suggested that the wings are produced during an early outburst of renewed activity of the nucleus, when the jet axis precesses; they noted that the low surface brightness of the wings, their steep radio spectrum, and the high degree of polarization could be explained in this way. One of the most popular present-day explanations of the nature of X-shape radio galaxies (below referred to as X-RG)

*E-mail: vo@sao.ru

is the interaction and merging of two supermassive black holes (SMBHs), which leads to a rapid change in the inclination of the spin axis of the central object and, as a consequence, the jet ejection direction (Merritt and Ekers 2002). As is shown in this paper, the orientation of the jet axis for an accreting black hole during the X-RG formation can change in a relatively short time interval, $<10^7$ yr. The direction of the SMBH spin axis can change rapidly even during its merging with objects whose masses are lower by an order of magnitude. In this model (Merritt and Ekers 2002), the second black hole (BH) has a lower mass and passes near the larger one at the center of the radio galaxy during galaxy merging. As a result, a binary system of BHs emitting gravitational waves is formed. During the coalescence of the objects and the absorption of the orbital angular momentum of the smaller object, the direction of the spin axis of the larger BH changes rapidly. Accordingly, the direction of the ejected jets perpendicular to the spin axis of the accretion disk, which, in turn, is perpendicular to the BH spin axis, also changes. According to the estimates by Merritt and Ekers (2002), even a small BH with a mass of 1/5 of the larger one in the pair can change the direction of the spin axis of the latter by 90° during their merging.

Note that the main way to increase the sample of S- and X-shape radio galaxies consists in investigating the images of radio sources recorded in sky surveys. In this study carried out within the framework of the project aimed at expanding the list of giant radio galaxies (GRGs), we detected eight new radio sources with signatures of interacting galaxies based on NVSS: three of them correspond to the X-RG class, four belong to the morphological S type whose S-shape is explained by the RG jet precession as a result of object merging, and one object belongs to double active nuclei. Thus, among the small class of GRGs and GRG candidates, there are objects demonstrating various merging stages. The GRG-class radio galaxies stand out among the radio sources by their large sizes, which are of the order of or more than 1 Mpc and are comparable to the sizes of galaxy clusters. Of the order of 200 GRGs with flux densities above 150 mJy at 1.4 GHz are known to date. As a rule, GRGs belong to the FR II morphological type (Fanaroff and Riley 1974) and are identified in the optical band with giant elliptical galaxies and quasars. GRGs are considerably less widespread than normal radio galaxies, which complicates their statistical study. Several groups (Schoenmakers et al. 2001, 2002; Lara et al. 2001, 2004; Saripalli et al. 2005; Konar et al. 2004, 2008; Jamrozy et al. 2005, 2008; Machalski et al. 2006; Komberg and Pashchenko 2009; Khabibullina et al. 2010, 2011a, 2011b) are involved in their study. As Jamrozy et al. (2005) pointed out, since the GRG sizes are comparable to or even larger than the sizes of galaxy groups, the existence of GRGs can affect significantly the environment.

Below, we describe new X–RG objects and S-shape radio galaxies found in the list of GRG candidates compiled by analyzing the structure of faint extended radio sources with angular sizes $>4'$ (Solovyov and Verkhodanov 2011, 2014a, 2014b) based on NVSS data (Condon et al. 1998). In Section 2, we present the technique for preparing the primary list. In Section 3, we describe the procedures and results of the radio and optical identifications of objects. The conclusions are presented in Section 4.

2. THE PROCEDURE FOR SELECTING RADIO GALAXIES

We selected the radio galaxies—candidates for objects with double active nuclei—based on NVSS (NRAO VLA Sky Surveys) maps (Condon et al. 1998) from the preliminary list of GRG candidates that contains 25 FR I sources and 30 FR II sources in its primary version (Solovyov and Verkhodanov 2011). The NVSS covers 82% of the celestial sphere (the entire sky north of 40° in declination) and has a fairly high angular resolution. The NVSS catalog contains ~1.81 million discrete objects at a frequency of 1.4 GHz. The flux density limit for a resolvable discrete source in the NVSS is 2.5 mJy. For objects with a surface brightness >15 mJy, the resolution accuracy is estimated to be $\leq 1''$. The selected GRG candidates in our list have higher flux densities. When selecting the candidates for extended giant sources, we assumed that they were at least two-component objects whose extended radio components were resolved and classified in the NVSS catalog as separate independent sources. When analyzing the catalog, we used procedures from the CATS database (Verkhodanov et al. 2005, 2009). The algorithm of searching for double sources uses four parameters:

- the angular distance between the centers of the sources d,
- the size of the source's major axis a in the NVSS catalog,
- the angle ϕ between the directions of the major axes of the pair of objects being checked,
- the integrated flux density of the source S_i.

The selection procedure allows us to choose the objects from the catalog that have extended structures elongated along a single line. The algorithm parameters were specified within the range $4' \leq d \leq 6'$, where the lower limit was chosen as the minimum scale on which our data could be compared with the highest spherical harmonics of the Planck CMB map and the upper limit was set by the characteristic distance between the extended components at a mean number of such objects $\sim$1000–1500 estimated from the surface density of the already cataloged sources (Verkhodanov et al. 2008). In addition, a standard quadratic increase in the number of objects in the field begins from $d \sim 6'$, which can lead to confusion and to selection effects that are difficult to take into account in the automatic procedure.

The angle between the major axes of the GRG candidate sources was chosen to be $\phi \leq 10^\circ$. This corresponds to the adopted alignment, for example, when discussing the conditions for the coincidence of the radio and optical axes in radio galaxies (Chambers et al. 1987; Pariiskii et al. 1996).

For our analysis, we used the sources with the sizes of the major and minor axes and the position angle measured in the NVSS. In the preliminary list, we included the objects (1) with $\phi \leq 10^\circ$ and/or (2) under the condition that the intersection of the extensions of the straight lines on which the semimajor axes of the analyzed objects of the studied pair lay was located at a distance from the sources than did not exceed the separation between the objects. Such a procedure allows us to identify the various morphologically related objects that can distort the result of the CMB component separation on the investigated angular scales. The selected objects were visually inspected to remove the erroneously chosen ones. For this purpose, we used the internal *nvsscat* NVSS image request procedure from the FADPS system (Verkhodanov 1997).

3. IDENTIFICATION

To check the identification and to search for the host galaxy candidates, we used the databases of optical surveys: the Digitized Palomar Sky Survey (DSS), the Space Telescope Science Institute (STScI), and the catalogs of the 2MASS infrared survey (2MASS Collaboration 2002; Cutri et al. 2002). In the radio identification, we used the CATS database[1] (Verkhodanov et al. 2005, 2009a). In calculating the spectral indices, we used the results of the cross-identification in the CATS database with a $180'' \times 180''$ identification window. To remove the accidental field radio objects in a given box, we used a data analysis technique similar to that described in Verkhodanov et al. (2000, 2009b). The essence of the method consists in applying a joint analysis of the data in coordinate and spectral spaces for the selection of probable identifications of specific radio sources at various radio frequencies. For this purpose, we used the *spg* code (Verkhodanov 1997b) from the RATAN-600 continuum data processing system. In describing the spectra $S(\nu)$ for the subsequent calculation of the spectral indices, we applied the parametrization of $S(\nu)$ by the formula $\log S(\nu) = A + Bx + Cf(x)$, where S is the flux density in Jy, x is the logarithm of the frequency ν in MHz, and $f(x)$ is one of the following functions: $\exp(-x)$, $\exp(x)$, or x^2.

The spectra were approximated when the flux density errors ΔS were specified in accordance with the following rule: for $\nu \geq 1.5$ GHz, the error ΔS_ν was set equal to $0.1S_\nu$ at $\Delta S_\nu^{\text{init}} < 0.1S_\nu$ or equal to that presented in the catalog at a lower measurement accuracy; for $\nu < 1.5$ GHz, $\Delta S_\nu = 0.15S_\nu$ at $\Delta S_\nu^{\text{init}} < 0.15S_\nu$ or equal to the initial one in the catalog at a lower accuracy. This approach allows us to reduce the influence (weight) of the low-frequency range of the spectrum, where additional systematic effects related to the large beam size of the radio telescope can manifest themselves when estimating the flux density.

The spectrum approximation results for the objects are presented in the table. The columns of the table give: (1) the IAU name including the coordinates of the source and the components; (2) the type of radio structure according to the classification of Fanaroff and Riley; (3) the flux density in mJy at 1.4 GHz; (4) the angular size in arcmins and the linear size in Mpc if the redshift is available; (5) the infrared (I) optical (O), and X-ray (X) identifications; (6) the redshift z; and (7) the continuum approximation function for the integrated flux density. Among the main radio catalogs of the CATS database used in constructing the spectra of the GRG candidates, we will point out the following lists: 3C (Bennett 1962), PKS (Bolton et al. 1964), 4C (Pilkington and Scott 1965), NVSS (Condon et al. 1998), Culgoora (Slee 1995), Texas (Douglas et al. 1996), FIRST (Becker et al. 1995), WISH (De Breuck et al. 2002), WENSS (Rengelink et al. 1997), GB6 (Gregory et al. 1996), the UTR catalog of deblended objects (Verkhodanov et al. 2003), 6C (Baldwin et al. 1985), 7C (McGilchrist et al. 1990), 8C (Hales et al. 1995), VLSS (Lane et al. 2012), PMN (Griffith et al. 1994), SUMSS (Mauch et al. 2003), B2 (Colla et al. 1970), and MRC (Large et al. 1991). The integrated continuum radio spectra of the identified objects constructed from multifrequency measurements are shown in Fig. 1.

[1] http://cats.sao.ru

Radio galaxies with signatures of merging from the list of GRG candidates detected by the method of comparing of the components' axes

Name	Type	$S_{1.4}$, mJy	Size, /Mpc	XIO	z	Spectrum
J005744.4+302156	S, FR I	586.8	8.4/0.17	XIO	0.0165	$3.155 - 1.296x + 0.120x^2$
J010725.4+322439	S, FR I	915.5	11.1/0.24	XIO	0.0170	$2.687 - 0.640x$
J015756.3+020950	X, FR II	350.3	8.7/–	IO		$3.845 - 1.326x$
J015745.3+021004		163.5				
J015807.4+020934		186.8				
J031821.9+682932	X, FR II	323.4	17.1/1.74	IO	0.0901	$3.581 - 1.222x$
J031747.1+682508		171.2				
J031802.4+682713		152.2				
J065122.5+193713	P, FR I/II	244.7	7.7/–	IO		$-2.581 + 2.612x - 0.562x^2$
J065114.6+193615		71.3				
J065130.5+193811		173.4				
J115909.1+582041	S, FR II	147.8	6.7/0.42	IO	0.0537	$0.491 - 0.001x - 0.038e^x$
J154901.7–321747	X, FR I/II	836.6	9.2/1.11	–	0.1082	$1.302 - 0.046e^x$
J154854.8–321557		389.3				
J154908.6–321938		447.3				
J210138.4–280158	S, FR I/II	2672.1	6.7/0.31	IO	0.0397	$3.288 - 0.812x$
J210139.5–280321		2054.6				
J210141.2–275830		707.5				

The columns of the table give the IAU names of the sources including the object coordinates, the type of radio structure according to the morphological signatures of interaction (S, X, or P (pair)) and according to the classification of Fanaroff and Riley, the flux density in mJy, the angular and linear (if the redshift z is known) sizes of the object, identification (X-ray (X), infrared (I), optical (O)), z, and the radio spectrum approximation curve.

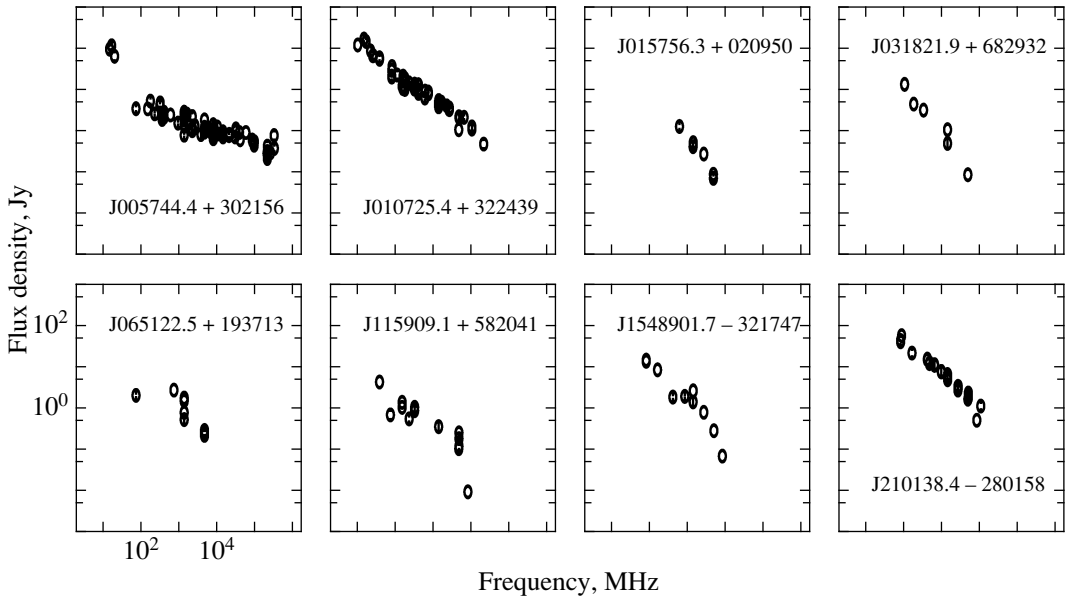

Fig. 1. Continuum radio spectra of the objects based on the identifications in CATS. The scale along the axes is logarithmic.

The structure of the radio galaxies is shown in Fig. 2. The images were constructed using the NVSS 1.4-GHz maps.

Comments to the Sources

The optical and infrared identifications of the GRG candidates were made by using the NED[2] (NASA/IPAC Extragalactic Database) and SkyView[3] databases and virtual observatories, which provide the tools for comparing the maps in different wavelength ranges. The optical and infrared identifications of the central object were made for the centroid of the integrated radio image. Below, we discuss the results of these identifications for objects in the databases as well as on the optical, infrared, and submillimeter maps.

J005744.4+302156. An FR I radio source with a characteristic brightness decline from the center to the edges of the structure and a high-contrast radio jet; it is identified in the optical band with the elliptical galaxy NGC 315 with an apparent magnitude of $11^m.2$. The radio source is present on the 100-GHz Planck map (Fig. 3). According to the results of its optical identification, the object has a linear size of ∼170 kpc, which excludes it from the GRG list.

J010725.4+322439. An FR I radio source with a characteristic radio brightness decline from the center to the edges of the structure; a multiple bending of the radio structure corresponding to the characteristic S-shape is observed. It is cataloged as 3C 31 and 4C+32.05. The host galaxy is NGC 383 ($12^m.14$). Details of the structure are also seen on the Planck maps at 100 GHz and on the CMB map (Fig. 4). According to the results of its identification, the object has a linear size of ∼240 kpc, which excludes it from the GRG list.

J015756.3+020950. A dumbbell-shaped FR II radio galaxy with a slightly fragmented structure closer to its center. Faint wings corresponding to X-morphology are observed at the center of the radio source. APMUKS B015517.56+015518.5 ($B = 20^m.08$) is a candidate for identification on the DSS image.

J031821.9+682932. An FR II radio galaxy with clearly separated radio components, one of which is brighter than the other. The brighter component closer to the center has a perpendicular small structure as one of the X-RG wings. The object is identified with the Seyfert galaxy 2MASX J03181899+6829322. According to the results of its identification, the object has a linear size of ∼1.74 Mpc, which confirms its classification as GRG.

J065122.5+193713. A radio galaxy with extended radio components elongated in the same direction (in the northeast in the equatorial coordinate system), with hot spots being present at their beginning. The structure of the object is typical of sources moving in the gas of a galaxy cluster. It is identified with the source 2MASX J06513590+1935513 ($V =$

[2] http://nedwww.ipach.caltech.edu
[3] http://skyview.gsfc.nasa.gov

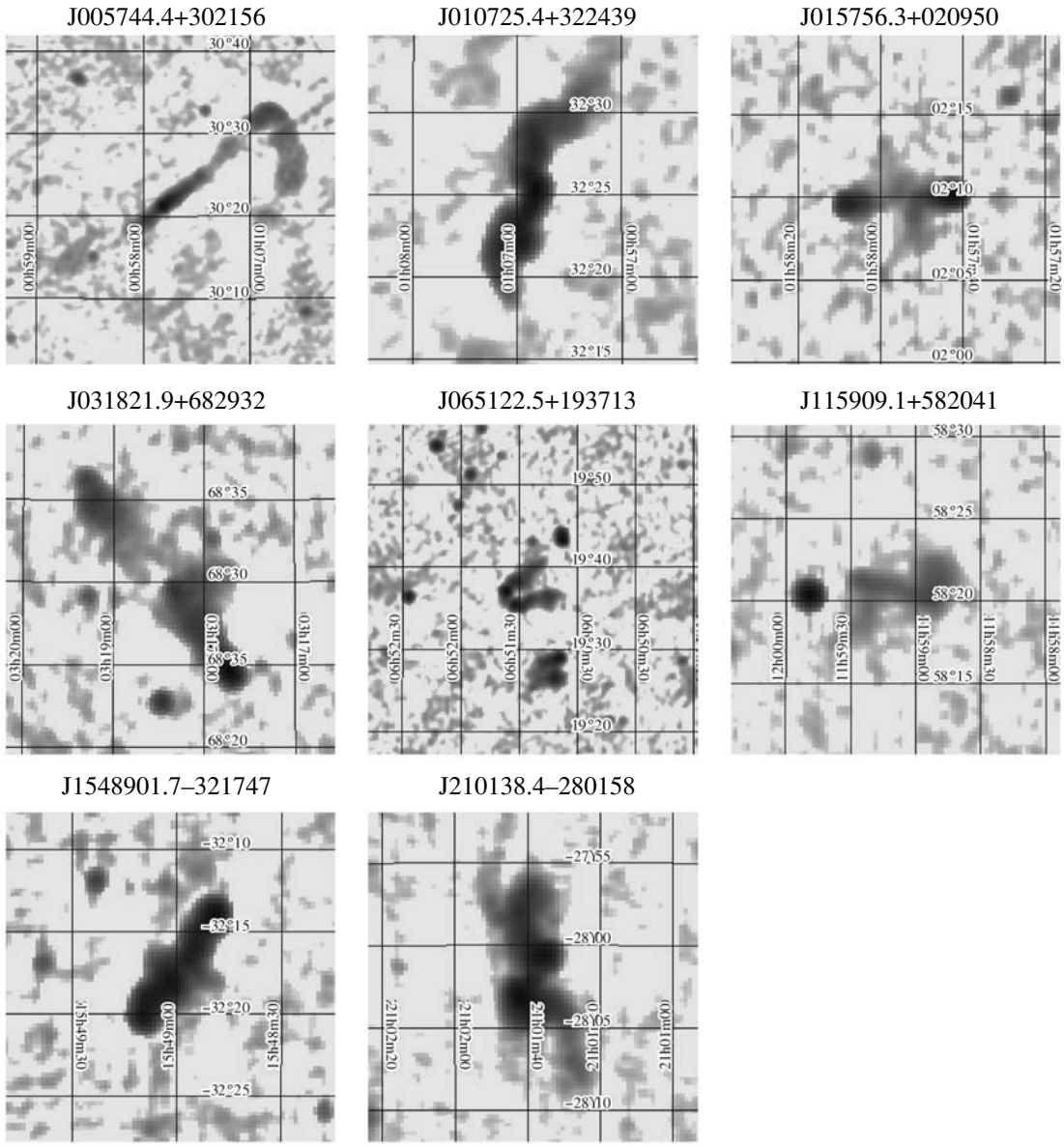

Fig. 2. Structure of the radio galaxies with signatures of interaction. The images were constructed using the NVSS 1.4-GHz maps.

$15\overset{m}{.}5$) located at the center of gravity between the hot spots. At 10′ to the southeast, there is the double source J065109.6+192852/J065112.1+192616 with extended components directed oppositely to the components of J065122.5+193713.

J115909.1+582041. An FR II radio galaxy with an indistinct dumbbell shape. Faint structures emanate from the radio components in opposite directions, which may suggest the rotation of the radio galaxy nucleus. The probable identification is CGCG 292-05 ($B = 15\overset{m}{.}7$).

J154901.7−321747. An FR II radio galaxy; it has a dumbbell shape typical of its class, except for the presence of yet another smaller extended structure crossing the center at an angle and having a decreasing radio brightness distribution with FR I. It can be classified as the separate "X" type. It is cataloged as PKS 1545-321. According to the results of its identification, the object has a linear size of ∼1.11 Mpc, which confirms its classification as GRG.

J210138.4−280158. An FR I radio source with a strongly bent radio structure with two prominent spots arranged symmetrically relative to the center. It has a typical spiral S-shape, is cataloged as

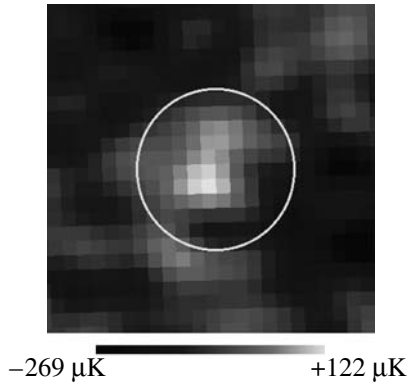

Fig. 3. The field centered on the radio galaxy J005744.4+302156 on the Planck map with the source. The observational data are at 100 GHz. The field size is $30' \times 30'$. The right ascension and declination are long the horizontal and vertical axes, respectively. The position of the radio galaxy is marked by the circle.

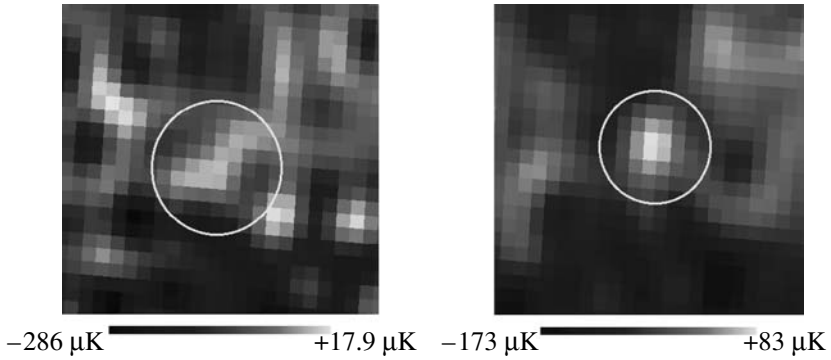

Fig. 4. The field centered on the radio galaxy J010725.4+322439 on the Planck maps with the source: (a) the observational data at 100 GHz and (b) the CMB data. The field size is $30' \times 30'$. The right ascension and declination are long the horizontal and vertical axes, respectively. The position of the radio galaxy is marked by the circle.

PKS 2058−282, and is identified with NGC 6998 (an apparent magnitude of $14^m.2$). According to the results of its identification, the object has a linear size of ∼310 kpc, which excludes it from the GRG list.

4. CONCLUSIONS

We presented the results of our search for and identification of eight radio galaxies with signatures of interaction from the list of giant radio galaxy candidates. The candidates were selected by the method of comparing the axes of the components in the "unassociated" NVSS radio sources with a separation larger than $4'$ (Solovyov and Verkhodanov 2011). For our study, we selected objects with a complex morphology. Among them, there are four objects that can be classified as S-shape radio galaxies (J010725.4+322439 and J210138.4−280158 have the most characteristic shapes). Three radio sources, J015756.3+020950, J031821.9+682932, and J154901.7−321747, were classified as X-shape radio galaxies representing a rather small but interesting group of radio sources with a hypothetically possible rapid change in the spin axis of the central object after the merging of the host galaxies and their nuclei. One of the double radio sources (J065122.5+193713) has a structure with aligned extended components suggesting a possible blow of the radio source by the cluster gas.

The identification was made in the optical, infrared, submillimeter, and radio bands. The response from the host galaxies of two radio objects is observed on the CMB maps, introducing an additional signal into these data.

Almost all radio galaxies exhibit a steep continuum spectrum constructed from the integral data in a wide radio frequency range. Two of the investigated radio galaxies (J005744.4+302156 and

J010725.4+322439) are visible on the 100-GHz CMB maps, with J010725.4+322439 being visible not only on the maps of the original data channel but also on the cleaned CMB map. For two sources, J031821.9+682932 and J154901.7−321747, we confirmed their belonging to the class of giant radio galaxies with a linear size >1 Mpc.

The detection of S- and X-shape galaxies using the developed technique of comparing the axes demonstrated new possibilities of searching for objects with signatures of interaction. The development of this technique and its inclusion in the the searching procedure with an additional axis can help in identifying new objects of this type. In addition, we continue our work on the identification and analysis of giant radio galaxies from the Planck millimeter and submillimeter maps; its results will be presented in our next publication.

ACKNOWLEDGMENTS

We wish to thank the referee for the remarks that allowed the text of the paper to be improved. In this study, we use the NASA/IPAC Extragalactic Database (NED) which is operated by the Jet Propulsion Laboratory, California Institute of Technology, under contract with the National Aeronautics and Space Administration and the SkyView virtual observatory. We also used the CATS database of radioastronomical catalogs (Verkhodanov et al. 2005, 2009) and the FADPS[4] radioastronomical data processing system (Verkhodanov et al. 1993; Verkhodanov 1997). We are also grateful to the ESA for the open access to the observations and data processing in the Planck Legacy Archive. To analyze the Planck maps, we used the GLESP package[5] (Doroshkevich et al. 2011). This study was supported by the Russian Foundation for Basic Research (project no. 13-02-00027-a).

REFERENCES

1. J. E. Baldwin, R. C. Boysen, S. E. G. Hales, J. E. Jennings, P. C. Waggett, P. J. Warner, and D. M. A. Wilson, Mon. Not. R. Astron. Soc. **217**, 717 (1985).
2. R. H. Becker, R. L. White, and D. J. Helfand, Astrophys. J. **450**, 559 (1995).
3. A. Bennett, Mem. R. Astron. Soc. **68**, 163 (1962).
4. J. Bolton, F. Gardner, and M. Mackey, Austral. J. Phys. **17**, 340 (1964).
5. C. de Breuck, Y. Tang, A. G. de Bruyn, H. Rottgering, and W. van Breugel, Astron. Astrophys. **394**, 59 (2002).
6. K. C. Chambers, G. K. Miley, and W. J. M. van Breugel, Nature **329**, 604 (1987).
7. G. Colla, C. Fanti, A. Ficarra, L. Formiggini, E. Gandolfi, G. Grueff, C. Lari, L. Padrielli, et al., Astron. Astrophys. Suppl. Ser. **1**, 281 (1970).
8. J. J. Condon, W. D. Cotton, E. W. Greisen, Q. F. Yin, R. A. Perley, G. B. Taylor, and J. J. Broderick, Astron. J. **115**, 1693 (1998).
9. C. Cotanyi, Mex. Astron. Astrofiz. **21**, 173 (1990).
10. R. M. Cutri, M. F. Skrutskie, S. Van Dyk, C. A. Beichman, J. M. Carpenter, T. Chester, L. Cambresy, T. Evans, et al., *Explanatory Supplement to the 2MASS Second Incremental Data Release* (2002); http://www.ipac.caltech.edu/2mass.
11. A. G. Doroshkevich, O. B. Verkhodanov, P. D. Naselsky, J. Kim, D. I. Novikov, V. I. Turchaninov, I. D. Novikov, L.-Y. Chiang, and M. Hansen, Int. J. Mod. Phys. **20**, 1053 (2011); arXiv:0904.2517.
12. J. N. Douglas, F. N. Bash, F. A. Bozyan, F. A. Bozyan, G. W. Torrence, and Ch. Wolfe **111**, 1945 (1996).
13. B. L. Fanaroff and J. M. Riley, Mon. Not. R. Astron. Soc. **167**, 31p (1974).
14. P. C. Gregory, W. K. Scott, K. Douglas, and J. J. Condon, Astrophys. J. Suppl. Ser. **103**, 427 (1996).
15. M. R. Griffith, A. E. Wright, B. F. Burke, and R. D. Ekers, Astrophys. J. Suppl. Ser. **90**, 179 (1994).
16. S. E. G. Hales, E. M. Waldram, N. Rees, and P. J. Warner, Mon. Not. R. Astron. Soc. **274**, 447 (1995).
17. R. W. Hunstead, H. S. Murdoch, J. J. Condon, and M. M. Phillips, Mon. Not. R. Astron. Soc. **207**, 55 (1984).
18. M. Jamrozy, J. Machalski, K. H. Mack, and U. Klein, Astrophys. J. **433**, 467 (2005).
19. M. Jamrozy, C. Konar, J. Machalski, and D. J. Saikia, Mon. Not. R. Astron. Soc. **383**, 525 (2008).
20. M. L. Khabibullina, O. V. Verkhodanov, M. Singh, et al., Astron. Rep. **54**, 571 (2010); arXiv:1009.4539.
21. M. L. Khabibullina, O. V. Verkhodanov, M. Singh, et al., Astron. Rep. **55**, 392 (2011a); arXiv:1108.3295.
22. M. L. Khabibullina, O. V. Verkhodanov, M. Singh, A. Pyria, S. Nandi, and N. V. Verkhodanova, Astrophys. Bull. **66**, 171 (2011b); arXiv:1108.4490.
23. B. V. Komberg and I. N. Pashchenko, Astron. Rep. **53**, 1086 (2009); arXiv:0901.3721.
24. C. Konar, D. J. Saikia, C. H. Ishwara-Chandra, and V. K. Kulkarni, Mon. Not. R. Astron. Soc. **355**, 845 (2004).
25. C. Konar, M. Jamrozy, D. J. Saikia, and J. Machalski, Mon. Not. R. Astron. Soc. **383**, 525 (2008).
26. W. M. Lane, W. D. Cotton, J. F. Helmboldt, and N. E. Kassim, Radio Sci. **47**, ID RS0K04 (2012).
27. L. Lara, I. Marquez, W. D. Cotton, L. Feretti, G. Giovannini, J. M. Marcaide, and T. Venturi, Astrophys. J. **378**, 826 (2001).
28. L. Lara, G. Giovannini, W. D. Cotton, L. Feretti, J. M. Marcaide, I. Marquez, and T. Venturi, Astrophys. J. **421**, 899 (2004).
29. M. I. Large, L. E. Cram, and A. M. Burgess, The Observatory **111**, 72 (1991).

[4] http://sed.sao.ru/~vo/fadps_e.html
[5] http://www.glesp.nbi.dk

30. J. P. Leahy and P. Parma, in *Proceedings of the 7th IAP Conference, From Beams to Jets, Institut d'Astrophysique de Paris, Paris, France, July 2–5, 1991* (Cambridge University Press, Cambridge, New York, NY, USA, 1992), p. 307.
31. J. P. Leahy and A. G. Williams, Mon. Not. R. Astron. Soc. **210**, 929 (1984).
32. F. K. Liu, Mon. Not. R. Astron. Soc. **347**, 1357 (2004).
33. J. Machalski, M. Jamrozy, S. Zola, and D. Koziel, Astrophys. J. **454**, 85 (2006).
34. T. Mauch, T. Murphy, H. J. Buttery, J. Curran, R. W. Hunstead, B. Piestrzynski, J. G. Robertson, and E. M. Sadler, Mon. Not. R. Astron. Soc. **342**, 1117 (2003).
35. M. M. McGilchrist, J. E. Baldwin, J. M. Riley, D. J. Titterington, E. M. Waldram, and P. J. Warner, Mon. Not. R. Astron. Soc. **246**, 110 (1990).
36. D. Merritt and R. Ekers, Science **297**, 1310 (2002); astro-ph/0208001.
37. M. Murgia, Astron. Astrophys. **380**, 102 (2001).
38. Yu. N. Parijskij, N. S. Soboleva, O. V. Verkhodanov, A. I. Kopylov, and O. P. Zhelenkova, Bull. SAO **40**, 125 (1996).
39. J. D. H. Pilkington and P. F. Scott, Mem. R. Astron. Soc. **69**, 183 (1965).
40. J. E. Pringle, Mon. Not. R. Astron. Soc. **281**, 357 (1996).
41. R. B. Rengelink, Y. Tang, A. G. de Bruyn, G. K. Miley, M. N. Bremer, H. J. A. Roettgering, and M. A. R. Bremer, Eclipt. Astron. Astrophys. **124**, 259 (1997).
42. L. Saripalli, R. W. Hunstead, R. Subrahmanyan, and E. Boyce, Astron. J. **130**, 896 (2005).
43. A. P. Schoenmakers, K. H. Mack, A. G. de Bruyn, H. J. A. Roettgering, U. Klein, and H. van der Laan, Astron. Astrophys. Suppl. Ser. **146**, 293 (2000).
44. A. P. Schoenmakers, A. G. de Bruyn, H. J. A. Roettgering, and H. van der Laan, Astrophys. J. **374**, 861 (2001).
45. O. B. Slee, Austral. J. Phys. **48**, 143 (1995).
46. D. I. Solovyov and O. V. Verkhodanov, Astrophys. Bull. **66**, 416 (2011).
47. D. I. Solovyov and O. V. Verkhodanov, Astrophys. Bull. **69**, 141 (2014).
48. D. I. Solovyov and O. V. Verkhodanov, Astron. Rep. **58**, 506 (2014).
49. L. S. Sparke and J. S. Gallagher, *Galaxies in the Universe* (Cambridge Univ. Press, 2000).
50. 2MASS Collab., *2MASS Second Incremental Data Release Catalogs and Tables* (2002).
51. O. V. Verkhodanov, ASP Conf. Ser. **125**, 46 (1997).
52. O. V. Verkhodanov, B. L. Erukhimov, M. L. Monosov, V. N. Chernenkov, and V. S. Shergin, Bull. SAO **36**, 132 (1993).
53. O. V. Verkhodanov, in *Problems of Modern Radio Astronomy, Proceedings of the 27th Radio Astronomical Conference* (Inst. Appl. Astron. RAS, St. Petersburg, 1997), Vol. 1, p. 322.
54. O. V. Verkhodanov, S. A. Trushkin, H. Andernach, and V. N. Chernenkov, ASP Conf. Ser. **322**, 46 (1997).
55. O. Verkhodanov, H. Andernach, and N. Verkhodanova, Bull. SAO **49**, 53 (2000); astro-ph/0008431.
56. O. V. Verkhodanov, N. V. Verkhodanova, and H. Andernach, Astron. Rep. **47**, 110 (2003).
57. O. V. Verkhodanov, S. A. Trushkin, H. Andernach, and V. N. Chernenkov, Bull. SAO **58**, 118 (2005); arXiv:0705.2959.
58. O. V. Verkhodanov, M. L. Khabibullina, M. Singh, A. Pirya, N. V. Verkhodanova, and S. Nandi, in *Proceedings of the International Conference on Problems of Practical Cosmology, St. Petersburg, Russia, 2008,* Ed. by Yu. V. Baryshev, I. N. Taganov, and P. Teerikorpi (Russian Geograph. Soc., St. Petersburg, 2008), Vol. 2, p. 247.
59. O. V. Verkhodanov, S. A. Trushkin, H. Andernach, and V. N. Chernenkov, Data Sci. J. **8**, 34 (2009a); arXiv:0901.3118.
60. O. Verkhodanov, N. Verkhodanova, and H. Andernach, Astrophys. Bull. **64**, 72 (2009b); arXiv:0902.0311.
61. T. Wang, H.-Y. Zhou, and X.-Bo Dong, Astron. J. **126**, 113 (2003).
62. A. Wirth, L. Smarr, and J. S. Gallagher, Astron. J. **87**, 602 (1982).
63. A. J. Young, A. S. Wilson, S. J. Tingay, and S. Heinz, Astrophys. J. **622**, 830 (2005).

Translated by G. Rudnitskii